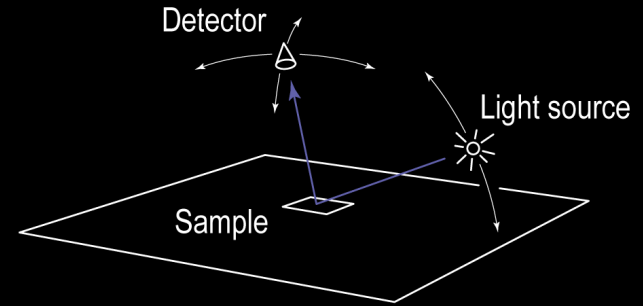


Interactive rendering with arbitrary BRDFs

Lecture 17

Full Gonioreflectometer

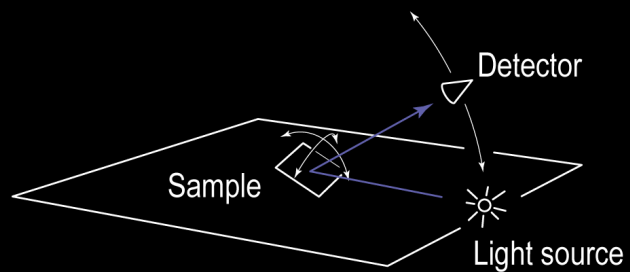
Straightforward 3D design



3 DOF: 2 detector, 1 source
Samples arranged on any desired grid

Full Gonioreflectometer

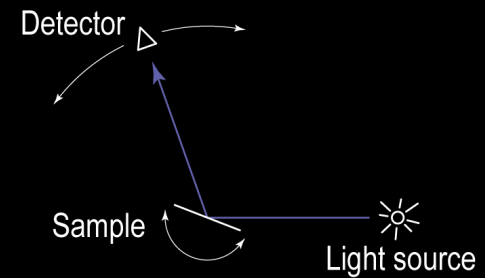
Alternate 3D design



3 DOF: 2 sample, 1 detector
Samples arranged on any desired grid

Incidence Plane

This conventional design...

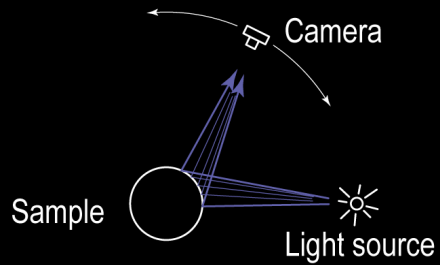


2 DOF: 1 detector, 1 sample
Samples arranged on any desired grid

Image-based Incidence Plane

...is equivalent to this image-based design

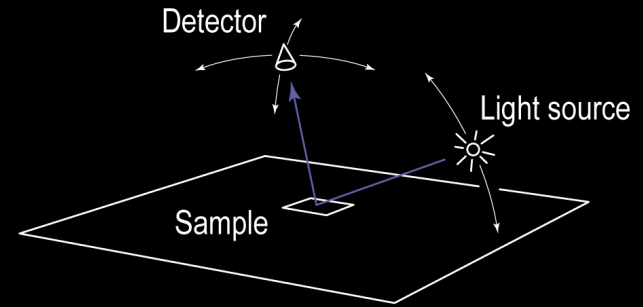
[Lu et al., AO '98]
[Marschner et al.,
AO '00]



2 DOF: 1 camera, 1 image
Samples arranged on predetermined curves

Full Gonioreflectometer

This conventional design...

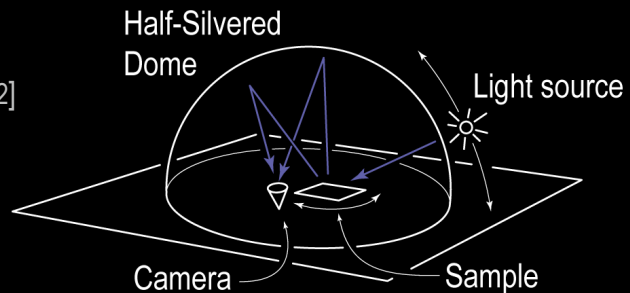


3 DOF: 2 detector, 1 source
Samples arranged on any desired grid

Image-based: Ward

...is equivalent to this image-based design

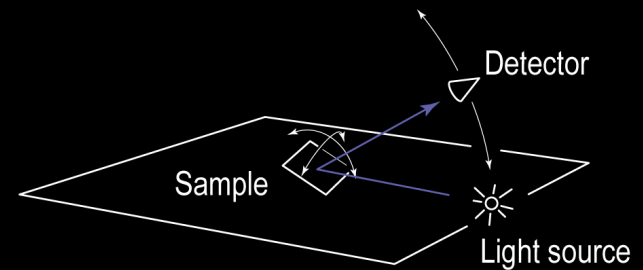
[Ward,
SG '92]



3 DOF: 2 image, 1 source (+1 sample)
Exitant directions fixed by optics; incident directions chosen

Full Gonioreflectometer

This conventional design...

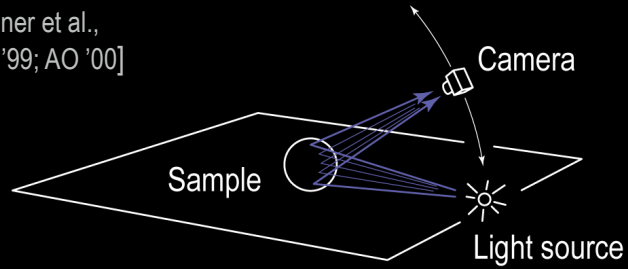


3 DOF: 2 sample, 1 detector
Samples arranged on any desired grid

Image-based: Marschner et al.

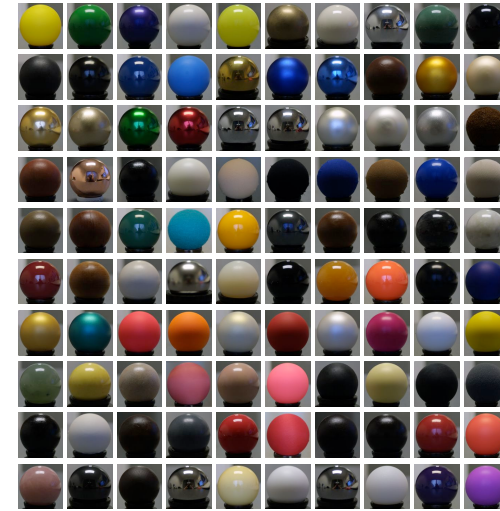
...is equivalent to this image-based design

[Marschner et al.,
EGRW '99; AO '00]



3 DOF: 2 image, 1 camera
Samples arranged on 2D sheets in 3D parameter space

MIT BRDF database



[Matusik et al. 2003]

Figure 5: Pictures of 100 of our acquired materials.

Rusinkiewicz parameterization

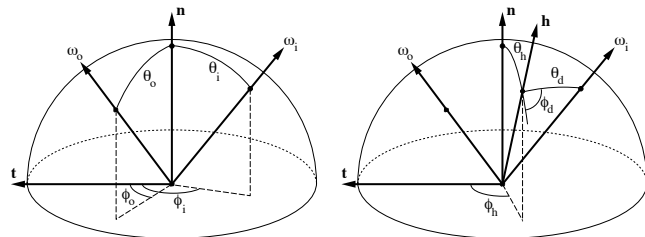
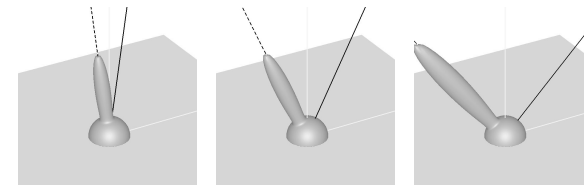


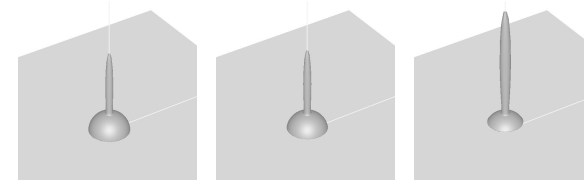
Figure 2: Proposed reparameterization of BRDFs. Instead of treating the BRDF as a function of (θ_i, ϕ_i) and (θ_o, ϕ_o) , as shown on the left, we consider it to be a function of the halfangle (θ_h, ϕ_h) and a difference angle (θ_d, ϕ_d) , as shown on the right. The vectors marked \vec{n} and \vec{t} are the surface normal and tangent, respectively.

[Rusinkiewicz 1998]



$\theta_i = 10^\circ$ $\theta_i = 20^\circ$ $\theta_i = 40^\circ$

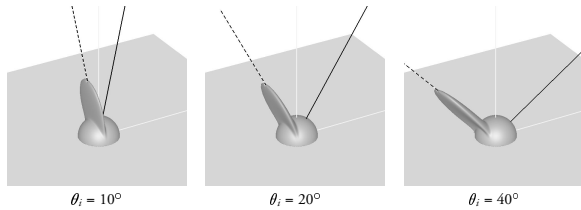
The Cook-Torrance-Sparrow BRDF seen as a function of (θ_i, ϕ_i) , for various values of (θ_i, ϕ_i) . Note that the position of the peak in space varies considerably.



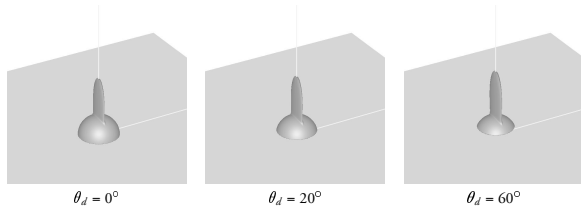
$\theta_d = 0^\circ$ $\theta_d = 20^\circ$ $\theta_d = 60^\circ$

The Cook-Torrance-Sparrow BRDF seen as a function of (θ_d, ϕ_d) , for various values of (θ_d, ϕ_d) . Note that although the size of the peak changes (as predicted by the Fresnel term), the position and shape of the peak remain constant. The BRDF is therefore approximated very closely by a function of the form $\beta = \beta_s(\theta_s)\beta_d(\theta_d)$, which means that only a small number of basis function coefficients will be nonzero.

[Rusinkiewicz 1998]

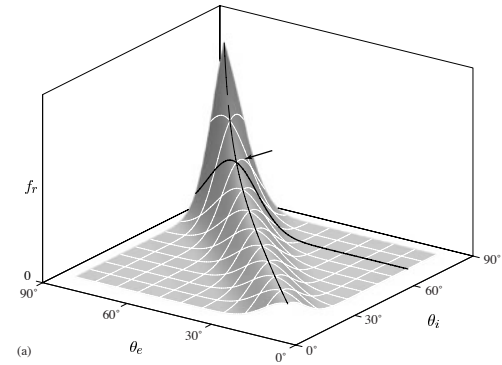


Ward's elliptical Gaussian BRDF seen as a function of (θ_e, ϕ_e) , for various values of (θ_i, ϕ_i) .

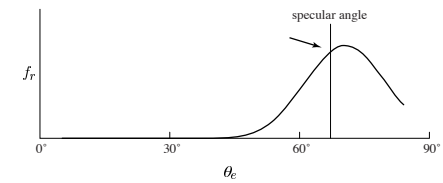


Ward's elliptical Gaussian BRDF seen as a function of (θ_e, ϕ_e) , for various values of (θ_i, ϕ_i) . The BRDF is very closely approximated by a function of the form $\beta = \beta_1(\theta_e)\beta_2(\phi_e)$.

[Rusinkiewicz 1998]



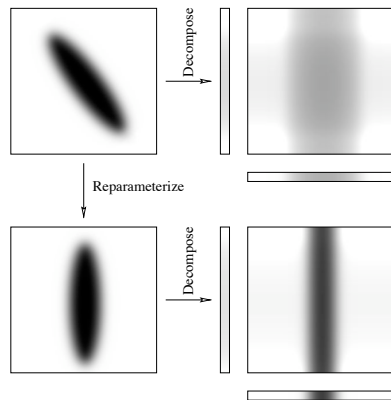
(a)



(b)

[Marschner 1998]

Separable approximation



[Kautz & McCool 1999]

Separable BRDF factorization

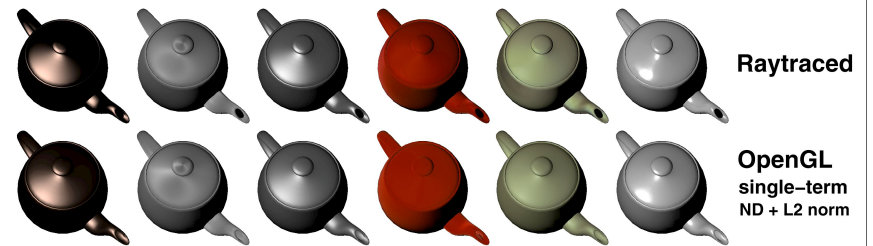
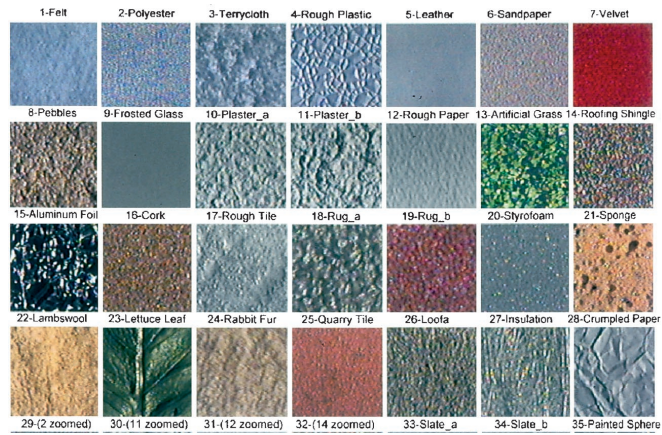


Figure 12: HTSG copper, Poulin/Fournier's brushed metal, Lafortune/Willems' modified Phong, measured velvet, measured peacock feather, and measured grey vinyl.

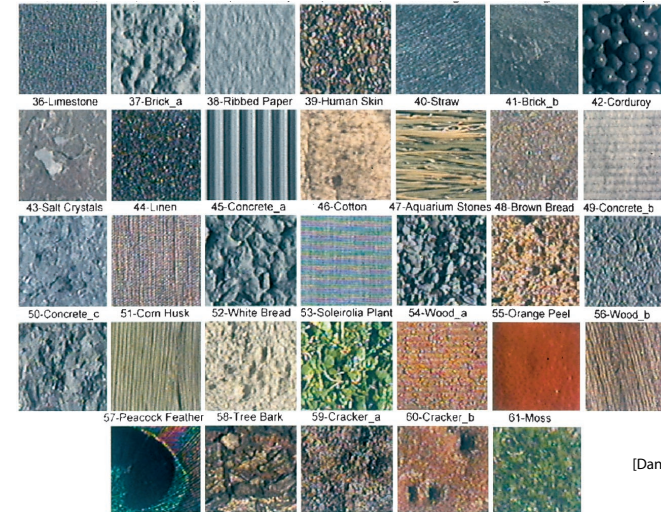
[Kautz & McCool 1999]

CURET BTF database



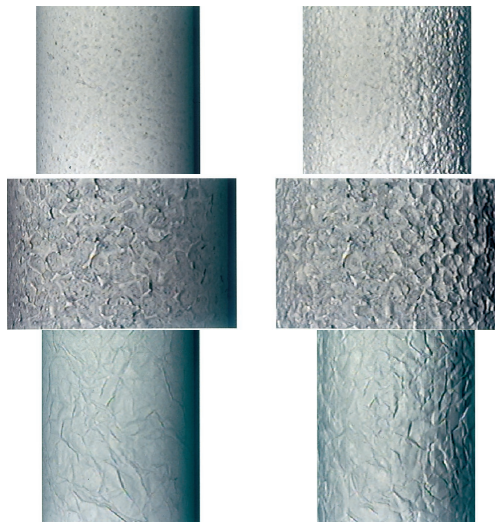
[Dana et al. 1999]

CURET BTF database



[Dana et al. 1999]

Rendering using BTF



[Dana et al. 1999]